SUPPLEMENTARY INFORMATION

Frankovský *et al*. The yeast mitochondrial succinylome: Implications for regulation of mitochondrial nucleoids

List of supplementary tables and figures

Table S1 (a separate *.xls file). **Summary of the mass-spec analysis of succinylated peptides using the MaxQuant 'match-between-runs' feature.**

Table S2 (a separate *.xls file). **List of proteins and Ksucc sites.** The table lists the (A) mitochondrial proteins and (B) succinylation sites detected in this study, together with (C) the union of the reference mitochondrial proteomes of Morgenstern et al. (2017), Vögtle et al. (2017) and Di Bartolomeo et al. (2020). The reference datasets of (D) the succinylome from Weinert et al. (2013) and (E) the acetylome from Henriksen et al. (2012) are also given. The overlaps between the datasets of the mitochondrial Ksucc proteins identified in this study with the (mitochondrial) succinylome of Weinert et al. (2013) and the (mitochondrial) acetylome of Henriksen et al. (2012) that served as the source for **Figure 2** are given in sheet S3F.

Table S3. Ratio of modified/unmodified lysine residues in recombinant Abf2p succinylated *in vitro*.

Table S4. **List of oligonucleotides.**

Figure S1. Linear Ksucc site sequence motifs. Sequence logos surrounding all Ksucc sites were generated using WebLogo 3.7.4 (Crooks et al., 2004) (A) and Seq2Logo 2.0 (Thomsen and Nielsen, 2012) (B). No amino acid in the surrounding of Ksucc site was enriched/depleted.

Figure S2. Ksucc detection with respect to lysine and protein abundance. The scatter plot for all succinylated proteins with more than one Ksucc site identified in this study. The vertical axis gives the Ksucc/K value and the horizontal axis shows the median molecules-per-cell count extracted from Ho et al. (2018). Mt-nucleoid proteins (SGD GO: 0042645) are circled in red. Proteins Tdh3, Fba1, Eno2, Tef1, Ssa2 and Tdh2 are omitted for scaling reasons because their molecules-per-cell count exceeds 130,000 but they were accounted-for in the analysis shown in **Figure S3**. All these proteins have major cytosolic functions (SGD).

Figure S3. Ksucc/K to molecules-per-cell values of mt-nucleoid proteins. The box plots show the distribution of the Ksucc/K to molecules-per-cell ratio for all proteins with more than one Ksucc site (n=223) and for mt-nucleoid proteins alone (SGD GO: 0042645). The red dot marks the average value, the median is indicated by the line between the grey and orange boxes. Median molecules-per-cell counts were extracted from Ho et al. (2018).

Figure S4. The inhibition of the DNA-binding activity of Abf2p is caused by its modification by succinylation and is not prevented by preincubation of the protein with DNA. (A) The inhibition of the DNA-binding activity of Abf2p is caused by its modification by succinylation, not by the mere presence of succinyl-CoA in the reaction mixture. When a reaction mixture containing 10 mM succinyl-CoA and Abf2p was gel filtrated on a Sephadex-G50 spin column (GE Healthcare) followed by a 3-hour incubation at 30°C, no inhibition of its DNA-binding activity was observed (lane 6). In contrast, when the reaction mixture was not gel-filtered (lane 8), incubation with 10 mM succinyl-CoA resulted in the inhibition of the

DNA-binding activity of Abf2p. (B) Preincubation with the DNA probe does not affect the inhibition of the Abf2p DNA-binding activity by succinylation. The succinylation of Abf2p (3-hours at 30°C) was performed either before (lanes 2 and 5) or after (lanes 3 and 6) a 10 min incubation with the *ScATP9* DNA probe.

Figure S5. Pre-incubation of Abf2p in the presence of 10 mM acetyl-CoA or acetylphosphate does not result in the inhibition of its DNA-binding activity *in vitro*. The incubation with succinyl-CoA, acetyl-CoA and acetylphosphate was performed for 3 hours at 30°C, followed by a 10 min incubation with the *ScATP9* DNA probe and EMSA.

Figure S6. Replacement of lysines (K) to arginines (R) in Abf2p results in its reduced ability to bind DNA *in vitro*. Increasing of the wild-type (WT) or mutant versions of Abf2p carrying substitution of a single (1xK-R), two (2xK-R) or three (3xK-R) lysines located in the PBBP regions of Abf2p (Figure 4A) were assessed for their DNA-binding activity by EMSA using radioactively labelled *ScATP9* as a probe.

Figure S7. The DNA-binding activities of mtHMG proteins from various yeast species exhibit different sensitivity to succinylation. Purified recombinant mtHMG proteins from *Saccharomyces cerevisiae* (*Sc*Abf2), *Yarrowia lipolytica* (*Yl*Mhb1), *Candida albicans* (*Ca*Gcf1) and *Candida parapsilosis* (*Cp*Gcf1) were incubated for 3 hours at 30°C in the presence of the indicated concentrations of succinyl-CoA and their DNA-binding activity was assessed by EMSA using radioactively labelled *ScATP9* as a probe.

Figure S8. Determination of un-succinylated (wt) and succinylated Abf2 (succ) molecular weight by size exclusion chromatography (SEC). Chromatographic comparison of the wild-type Abf2p (red) and succinylated Abf2p (blue). The samples were separated on a Superdex 75 10/300 GL column (GE Healthcare) equilibrated in 50 mM ammonium acetate, pH 7.3, 500 mM KCl, 5% (v/v) glycerol. The SEC elution profiles are normalized.

Figure S9. Mitochondrial nucleoids undergo changes during the diauxic shift. The strain *S. cerevisiae* SCY325 was inoculated at density of OD_{600} 0.2 into YPD medium. The growth was monitored by measuring OD_{600} and simultaneously the glucose levels were determined as described by Somogyi et al. (1952). Cells from a 3 l culture were collected by centrifugation (3000 × *g* for 20 min at 4°C) at the indicated time points corresponding to the log (fermentative), diauxic and stationary (respiratory) phase. Mitochondrial nucleoids were stained with DAPI (final concentration of 2.5 µg/ml) for 1 hour, washed with 10 mM Tris-HCl pH 7.6 and observed using a confocal microscope (Olympus IX81). Mitochondrial nucleoids were quantified as described below the legend. Bars represent standard error of means (SEM).

Quantification of mt-nucleoids (see bottom of the legend to Figure S9)

Supplementary references

Table S3. Ratio of modified/unmodified lysine residues in recombinant Abf2p succinylated *in vitro*.

Position within protein the full-length Abf2p	% of Ksucc
40	100.0
63	82.4
75	17.6
80	18.1
89	3.8
91	4.3
97	96.0
98	40.5
105	59.4
107	84.9
108	27.4
113	5.1
117	4.2
118	11.2
125	7.4
141	22.2
148	0.3
153	23.2
162	0.4
164	6.4
170	8.0
171	28.6

Table S4. List of oligonucleotides.

Name	Sequence (5'-3')	Template	Application
ScATP9_20_D	GGAGCAGGTATTGGTATTGC	Genomic DNA W303-1A	Preparation of probe for EMSA
ScATP9_50_R	ACACCATTAATTAAAGCTGC	Genomic DNA W303-1A	Preparation of probe for EMSA
Abf2_K162R_fwd	CGGGACAAATACATACAAGAG	pGEX-6P-2-ScABF2noMP	Construction of Abf2-K162R
Abf2_K162E_fwd	GACGACAAATACATACAAGAC	pGEX-6P-2-ScABF2noMP	Construction of Abf2-K162E
Abf2_K162_rev	AATGCTTTGATCCAAGGATTG	pGEX-6P-2-ScABF2noMP	Construction of Abf2-K162R and Abf2-K162E
LSC1_DC_LEU2_F	CGATTTCATAGAAAATTTCTTTTGCAGACCATTTAT TCTTCAGTTTGATAGAATTGTGTAGAATTGCAGATTC	Genomic DNA from the strain GG595; the sequence from the 5′ upstream region (670–693 bp from the START codon) of *LEU2* is underlined	Deletion cassette for construction of *lsc1*Δ strain
LSC1_DC_LEU2_R	AGACATAGAAGTCTTCCTCTTTTGAAAGCAGTTCATT CTCTTCCTAATATAACCATCAGATTTGGTATTGGTAG	Genomic DNA from the strain GG595; the sequence from the 3′ downstream region (497–519 bp from the STOP codon) of *LEU2* is underlined	Deletion cassette for construction of *lsc1*Δ strain
pLEU2_3_F	ATATTGACAAGGAGGAGGG	Colonies of *S. cerevisiae* SCY325 *lsc1*Δ	*lsc1*Δ genotype verification
pLSC1_3_R	AGGATAAATGAATATATACAAAGGG	Colonies of *S. cerevisiae* SCY325 *lsc1*Δ	*lsc1*Δ genotype verification
pLSC1_5_F	CAAATAAGTCATCTTGCACG	Colonies of *S. cerevisiae* SCY325 *lsc1*Δ	*lsc1*Δ genotype verification
pLEU2_5_R	TGAGAACATTCATGATTAGAGG	Colonies of *S. cerevisiae* SCY325 *lsc1*Δ	*lsc1*Δ genotype verification

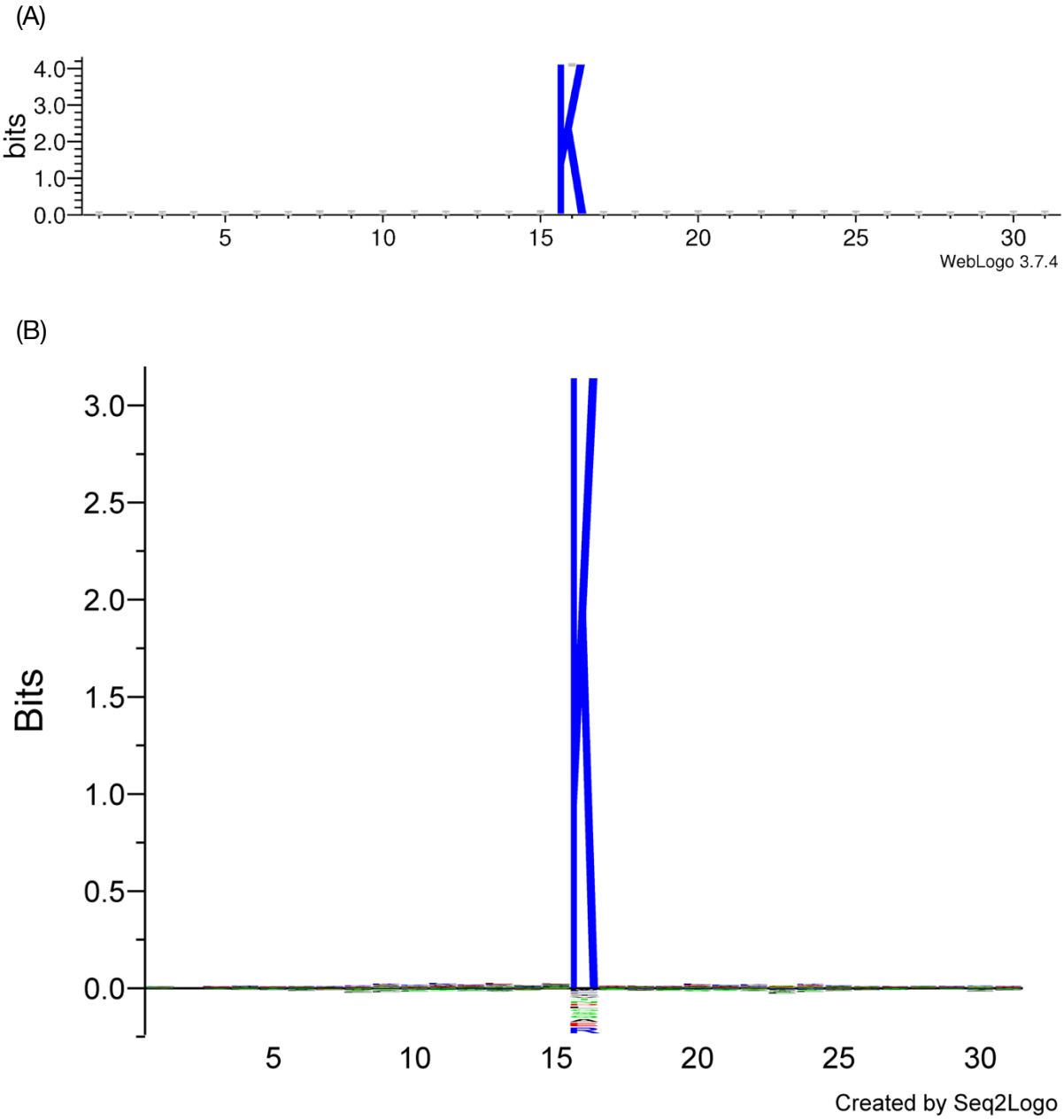

Figure S1. Linear Ksucc site sequence motifs. Sequence logos of regions surrounding all Ksucc sites (+/- 15 aa) were generated using WebLogo 3.7.4 (Crooks et al., 2004) (A) and Seq2Logo 2.0 (Thomsen and Nielsen, 2012) (B). No amino acid in the surrounding of Ksucc site was enriched.

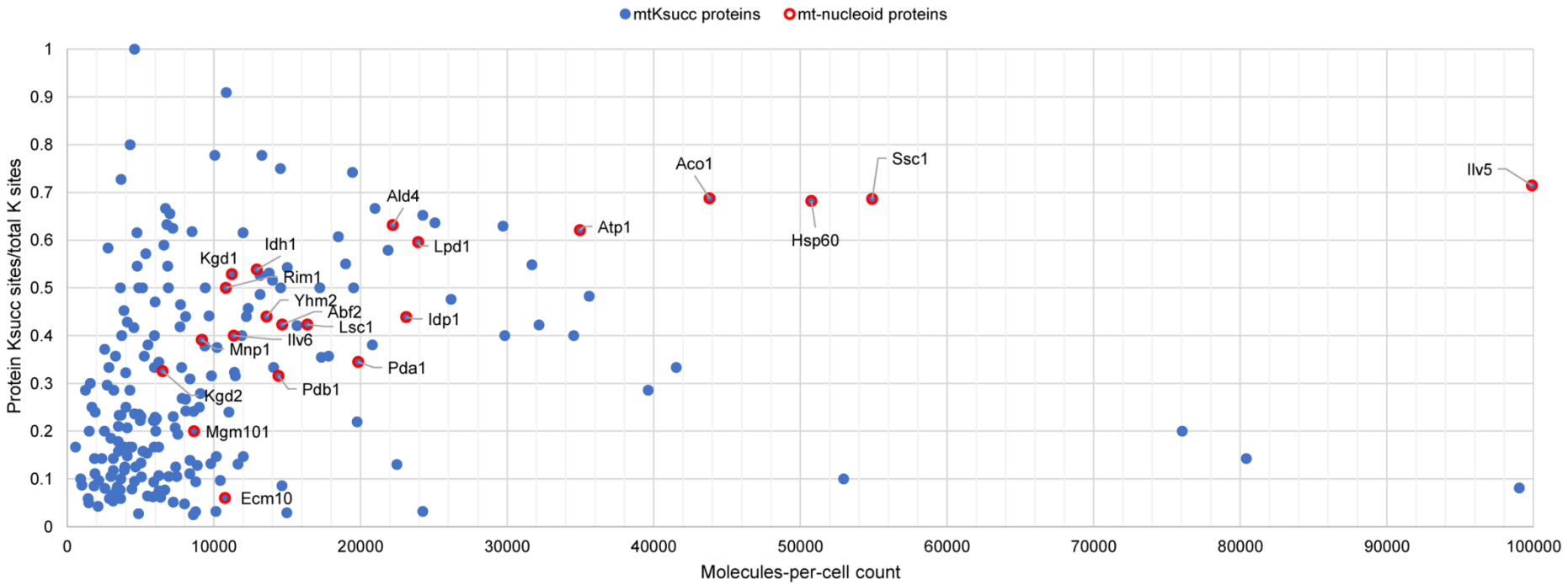

Figure S2. Ksucc detection with respect to lysine and protein abundance. The scatter plot for all succinylated proteins with more than one Ksucc site identified in this study. The vertical axis gives the Ksucc/K value and the horizontal axis shows the median molecules-per-cell count extracted from (Ho et al., 2018). Mt-nucleoid proteins (SGD GO: 0042645) are circled in red. Proteins Tdh3, Fba1, Eno2, Tef1, Ssa2, Tdh2, and Hsc82 are omitted for scaling reasons because their molecules-per-cell count exceeds 130,000 but they were accounted-for in the analysis shown in **Figure S3**. All these proteins have major cytosolic functions (SGD).

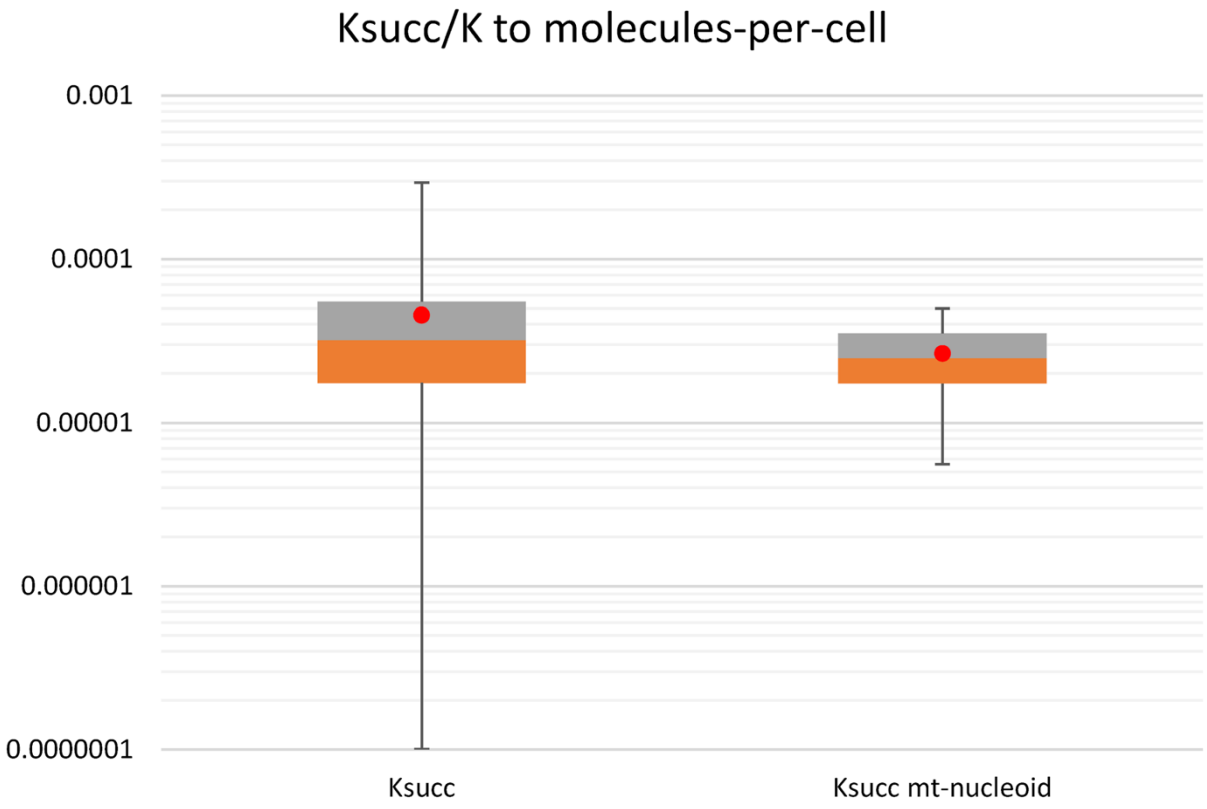

Figure S3. Ksucc/K to molecules-per-cell values of mt-nucleoid proteins. The box plots show the distribution of the Ksucc/K to molecules-per-cell ratio for all proteins with more than one Ksucc site (n=223) and for mt-nucleoid proteins alone (SGD GO: 0042645). The red dot marks the average value, the median is indicated by the line between the grey and orange boxes. Median molecules-per-cell counts were extracted from Ho et al. (2018).

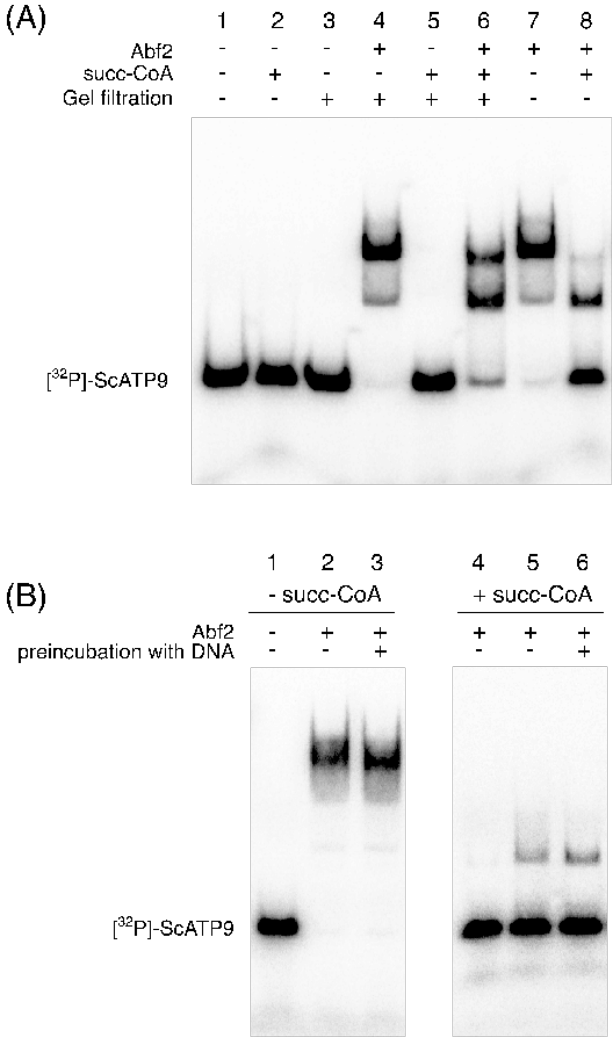

Figure S4. The inhibition of the DNA-binding activity of Abf2p is caused by its modification by succinylation and is not prevented by preincubation of the protein with DNA. (A) The inhibition of the DNA-binding activity of Abf2p is caused by its modification by succinylation, not by the mere presence of succinyl-CoA in the reaction mixture. When a reaction mixture containing 10 mM succinyl-CoA and Abf2p was gel filtrated on a Sephadex-G50 spin column (GE Healthcare) followed by a 3-hour incubation at 30°C, no inhibition of its DNA-binding activity was observed (lane 6). In contrast, when the reaction mixture was not gel-filtered (lane 8), incubation with 10 mM succinyl-CoA resulted in the inhibition of the DNA-binding activity of Abf2p. (B) Preincubation with the DNA probe does not affect the inhibition of the Abf2p DNA-binding activity by succinylation. The succinylation of Abf2p (3-hours at 30°C) was performed either before (lanes 2 and 5) or after (lanes 3 and 6) a 10 min incubation with the *ScATP9* DNA probe.

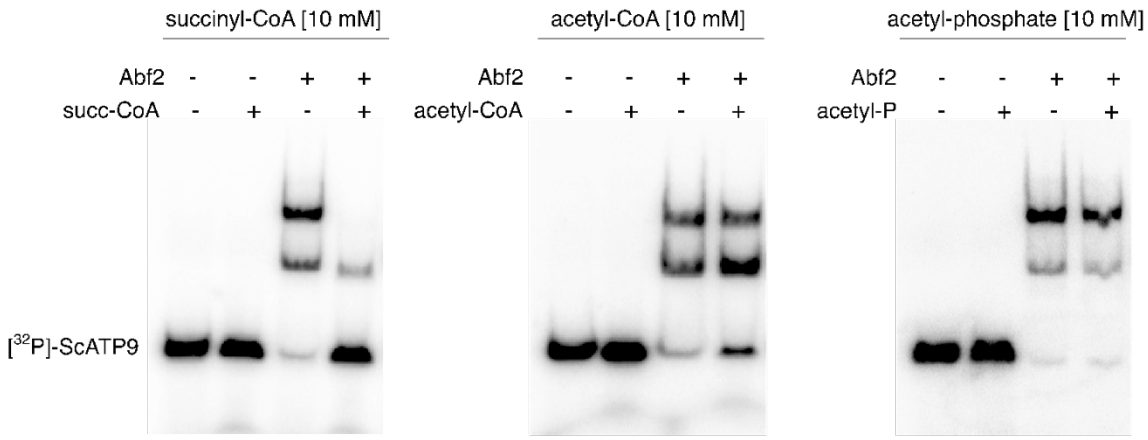

Figure S5. Pre-incubation of Abf2p in the presence of 10 mM acetyl-CoA or acetylphosphate does not result in the inhibition of its DNA-binding activity *in vitro*. The incubation with succinyl-CoA, acetyl-CoA and acetylphosphate was performed for 3 hours at 30°C, followed by a 10 min incubation with the *ScATP9* DNA probe and EMSA.

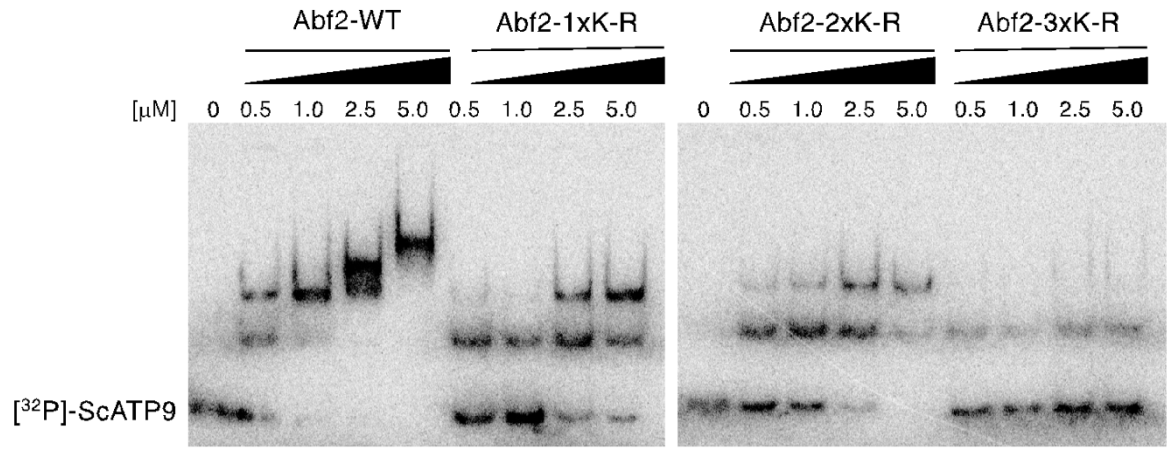

Figure S6. Replacement of lysines (K) to arginines (R) in Abf2p results in its reduced ability to bind DNA *in vitro*. Increasing of the wild-type (WT) or mutant versions of Abf2p carrying substitution of a single (1xK-R), two (2xK-R) or three (3xK-R) lysines located in the PBBP regions of Abf2p (Figure 4A) were assessed for their DNA-binding activity by EMSA using radioactively labelled *ScATP9* as a probe.

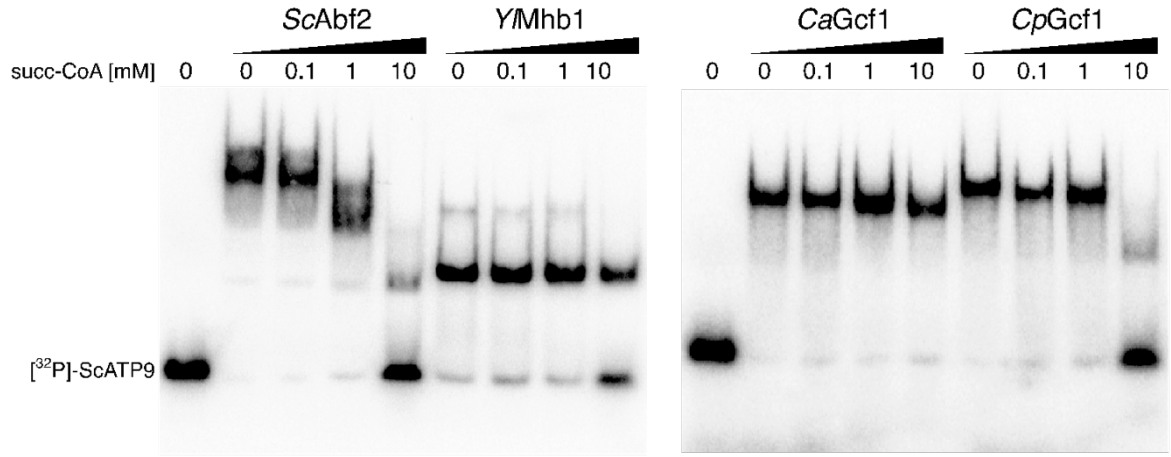

Figure S7. The DNA-binding activities of mtHMG proteins from various yeast species exhibit different sensitivity to succinylation. Purified recombinant mtHMG proteins from *Saccharomyces cerevisiae* (*Sc*Abf2), *Yarrowia lipolytica* (*Yl*Mhb1), *Candida albicans* (*Ca*Gcf1) and *Candida parapsilosis* (*Cp*Gcf1) were incubated for 3 hours at 30°C in the presence of the indicated concentrations of succinyl-CoA and their DNA-binding activity was assessed by EMSA using radioactively labelled *ScATP9* as a probe.

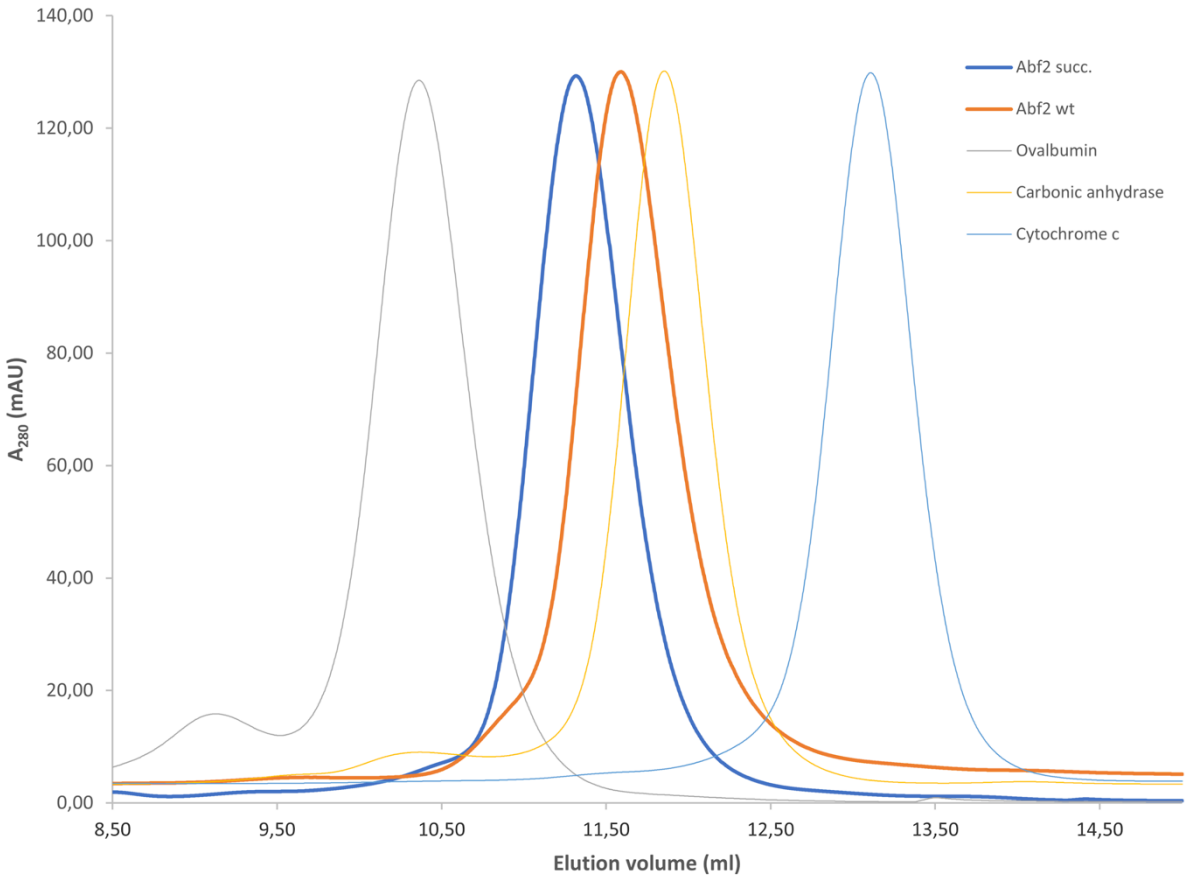

Figure S8. Chromatographic comparison of un-succinylated (wt) and succinylated Abf2p by a size-exclusion chromatography (SEC). Chromatographic comparison of the wild-type Abf2p (orange) and succinylated Abf2p (blue). The samples were separated on a Superdex 75 10/300 GL column (GE Healthcare) equilibrated in 50 mM ammonium acetate, pH 7.3, 500 mM KCl, 5% (v/v) glycerol. The SEC elution profiles are normalized. Ovalbumin (45 kDa), carbonic anhydrase (29 kDa) and cytochrome c (12 kDa) were used as Mw standards.

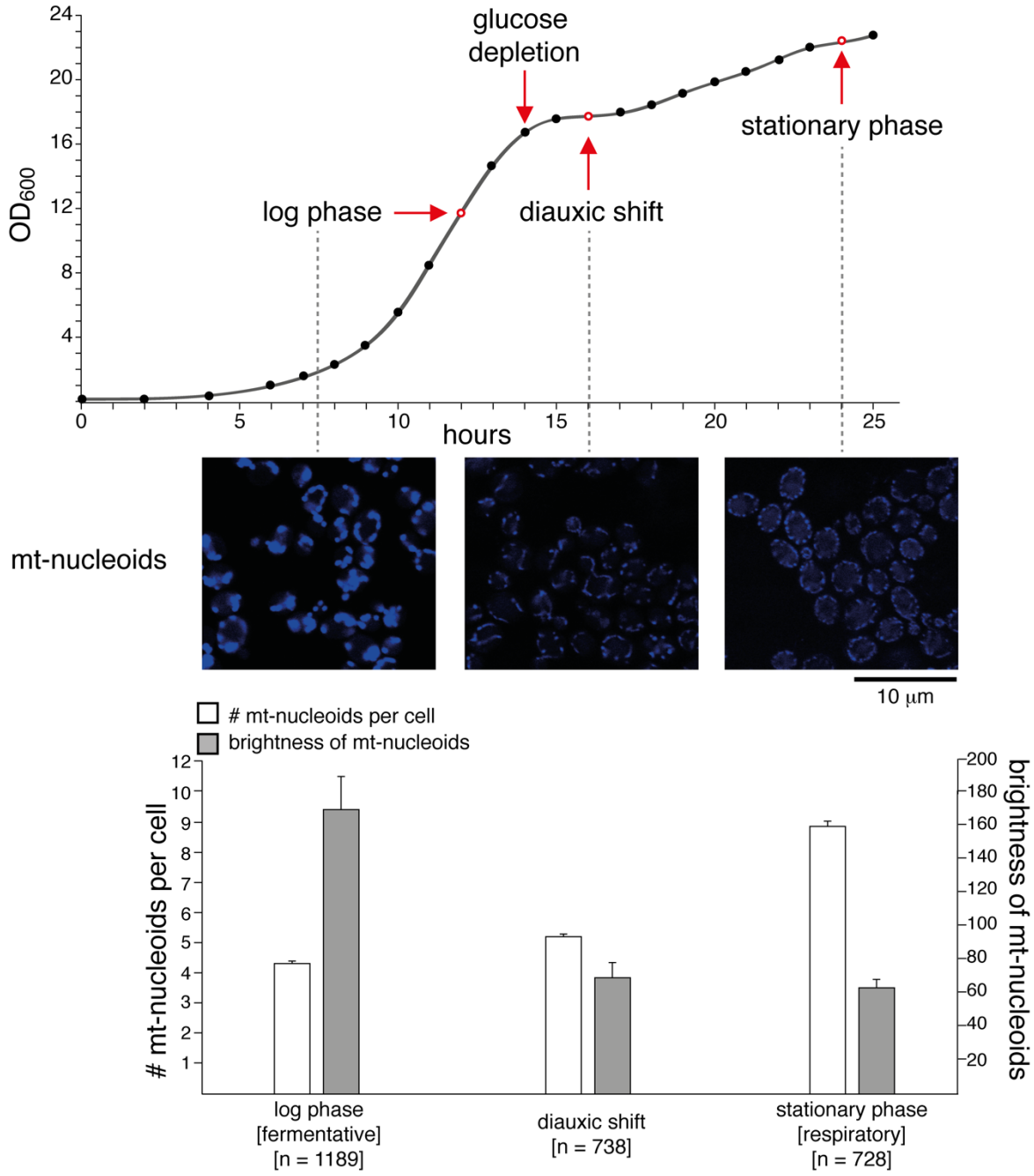

Figure S9. Mitochondrial nucleoids undergo changes during the diauxic shift. The strain *S. cerevisiae* SCY325 was inoculated at density of OD_{600} 0.2 into YPD medium. The growth was monitored by measuring OD_{600} and simultaneously the glucose levels were determined as described by Somogyi et al. (1952). Cells from a 3 l culture were collected by centrifugation (3000 × *g* for 20 min at 4°C) at the indicated time points corresponding to the log (fermentative), diauxic and stationary (respiratory) phase. Mitochondrial nucleoids were stained with DAPI (final concentration of 2.5 µg/ml) for 1 hour, washed with 10 mM Tris-HCl pH 7.6 and observed using a confocal microscope (Olympus IX81). Mitochondrial nucleoids were quantified as described below. Bars represent standard error of means (SEM).

Quantification of mt-nucleoids

Imaging data was segmented using cellpose (napari https://napari.org/index.html GUI plugin version) (Stringer et al., 2021). The widefield channel containing cells was segmented using the 'cyto' model with diameter set to 40. The blue channel was segmented using the 'nuclei' model with diameter set to 6. Resulting segmentation maps were inspected and thresholds were adjusted for optimal labelling. Labelled masks were imported into matlab for further analysis. Cells sharing a pixel with the border of the FOV were censored since they were likely incomplete. For each cell the number of compartments resulting from blue channel segmentation was determined. The average intensity of signal within these compartments was computed for every cell along with its standard deviation. SEM for the average intensity was obtained as standard deviation divided by square root of number of compartments. Data was analysed for each cell within the dataset and mean values were calculated per condition. Mean number of compartments along with its standard deviation were computed for every condition from the accumulated data. The SEM of compartment number was calculated as its standard deviation divided by the number of analysed cells.

The code used for the analysis:

```
clear
list_dirs = dir('**/*BL.tif*');
path = pwd;
frame = single(zeros(640,640));
frame(1:end,1) = 1;
frame(1,1:end) = 1;
frame(1:end,end) = 1;
frame(end,1:end) = 1;
counter = 0;
for ix = 1:length(list_dirs)
    cd(list_dirs(ix).folder)
    BL = single(ScanImageTiffReader('BL.tif').data());
    CL = single(ScanImageTiffReader('CL.tif').data());
    beads = single(ScanImageTiffReader('beads.tif').data());
    beads = permute(beads,[2,3,1]);
    beads(:,:,1:2)=[];

    nCells = max(CL(:))
    tempLabels = unique(CL(:));
    tempLabels(tempLabels==0)=[];
    nCells = length(tempLabels)
    if nCells > 500
        keyboard
    end
    for ix2 = 1:nCells
        tempCL = CL;
        tempCL(tempCL~=tempLabels(ix2)) = 0;
        check = tempCL .* frame;
        if max(check(:)) > 0
        else
            tempCL(tempCL>0) = 1;
            tempBL = BL .* tempCL;
            counter = counter+1
            nBeads(counter) = length(unique(tempBL(:))) - 1;
            tempBL(tempBL>0) = 1;
```

```
            tempBeads = beads .* tempBL;
            pixs = tempBeads(tempBeads~=0);
            meanIntensity(counter) = mean(pixs,'omitnan');
            sDev(counter) = nanstd(pixs);
            semInt(counter)=sDev(counter)/sqrt(nBeads(counter));


        end

    end
end
mmInt = mean(meanIntensity,'omitnan')
mmStd = mean(sDev,'omitnan')
mmBeads = mean(nBeads,'omitnan')
mmSem = mean(semInt,'omitnan')
semNB = nanstd(nBeads)/sqrt(counter);

cd(path)
save('glukozova.mat','nBeads','sDev','meanIntensity','mmInt','mmStd','mmBea
ds','mmSem','semNB')
```

Supplementary references

Di Bartolomeo, F., Malina, C., Campbell, K., Mormino, M., Fuchs, J., Vorontsov, E., Gustafsson, C.M., and Nielsen, J. (2020). Absolute yeast mitochondrial proteome quantification reveals trade-off between biosynthesis and energy generation during diauxic shift. Proc. Natl. Acad. Sci. USA *117*, 7524–7535.

Crooks, G.E., Hon, G., Chandonia, J.M., and Brenner, S.E. (2004). WebLogo: A sequence logo generator. Genome Res. *14*, 1188–1190.

Henriksen, P., Wagner, S.A., Weinert, B.T., Sharma, S., Bačinskaja, G., Rehman, M., Juffer, A.H., Walther, T.C., Lisby, M., and Choudhary, C. (2012). Proteome-wide analysis of lysine acetylation suggests its broad regulatory scope in *Saccharomyces cerevisiae*. Mol. Cell. Proteomics *11*, 1510–1522.

Ho, B., Baryshnikova, A., and Brown, G.W. (2018). Unification of protein abundance datasets yields a quantitative *Saccharomyces cerevisiae* proteome. Cell Syst. *6*, 192–205.

Morgenstern, M., Stiller, S.B., Lübbert, P., Peikert, C.D., Dannenmaier, S., Drepper, F., Weill, U., Höß, P., Feuerstein, R., Gebert, M., et al. (2017). Definition of a high-confidence mitochondrial proteome at quantitative scale. Cell Rep. *19*, 2836–2852.

Somogyi, M. (1952) Notes on sugar determination. *J. Biol. Chem.* **195**, 19–23.

Stringer, C., Wang, T., Michaelos, M., Pachitariu, M. (2021). Cellpose: a generalist algorithm for cellular segmentation. Nat. Methods *8*, 100-106.

Thomsen, M.C.F., and Nielsen, M. (2012). Seq2Logo: A method for construction and visualization of amino acid binding motifs and sequence profiles including sequence weighting, pseudo counts and two-sided representation of amino acid enrichment and depletion. Nucleic Acids Res. *40*, W281–W207.

Vögtle, F.N., Burkhart, J.M., Gonczarowska-Jorge, H., Kücükköse, C., Taskin, A.A., Kopczynski, D., Ahrends, R., Mossmann, D., Sickmann, A., Zahedi, R.P., et al. (2017).

Landscape of submitochondrial protein distribution. Nat. Commun. *8*, 1–10.

Weinert, B.T., Schölz, C., Wagner, S.A., Iesmantavicius, V., Su, D., Daniel, J.A., and Choudhary, C. (2013). Lysine succinylation is a frequently occurring modification in prokaryotes and eukaryotes and extensively overlaps with acetylation. Cell Rep. *4*, 842–851.